NANO LETTERS

2009
Vol. 9, No. 9
3100-3105

Free-Standing Epitaxial Graphene

Shriram Shivaraman,* Robert A. Barton, Xun Yu, Jonathan Alden, Lihong Herman, MVS Chandrashekhar, Jiwoong Park, Paul L. McEuen, Jeevak M. Parpia, Harold G. Craighead, and Michael G. Spencer

Cornell Center for Materials Research, Cornell University, Ithaca New York 14853

Received February 13, 2009; Revised Manuscript Received June 27, 2009

ABSTRACT

We report on a method to produce free-standing graphene sheets from epitaxial graphene on silicon carbide (SiC) substrate. Doubly clamped nanomechanical resonators with lengths up to 20 μm were patterned using this technique and their resonant motion was actuated and detected optically. Resonance frequencies of the order of tens of megahertz were measured for most devices, indicating that the resonators are much stiffer than expected for beams under no tension. Raman spectroscopy suggests that the graphene is not chemically modified during the release of the devices, demonstrating that the technique is a robust means of fabricating large-area suspended graphene structures.

Graphene is a two-dimensional crystal of carbon atoms arranged in a honeycomb lattice. It is a zero band gap semimetal with very unique electronic and optical properties including extremely high carrier mobilities, room temperature quantum Hall effect, and plasmon amplification, to name a few.[1−3] This has led to a tremendous rise in theoretical and experimental research investigating graphene for applications such as ultra-high-speed field-effect transistors, p−n junction diodes, terahertz oscillators, and low-noise electronic and optical sensors.[3−7] Graphene also has excellent mechanical properties and is a leading contender for nanoelectromechanical systems (NEMS). Graphene's Young's modulus is ∼1 TPa,[8] which is at least six times that of silicon. The strong in-plane bonding coupled with the weak interplanar van der Waals interaction makes it possible to fabricate extremely thin resonators, down to the limit of a single monolayer. Also, the chemical inertness of graphene makes it well suited for routine lithographic processing.

Epitaxial growth on silicon carbide (SiC) is a very promising method for large-scale production of graphene. In this method, single crystal SiC substrates are heated in vacuum to high temperatures in the range of 1200−1600 °C. Since the sublimation rate of silicon is higher than that of carbon, excess carbon is left behind on the surface, which rearranges to form graphene. In order to study the properties of epitaxially grown graphene, it would be beneficial to isolate the graphene from the substrate. For example, it has been reported that the electronic mobility of suspended exfoliated graphene is ∼10 times larger than that of exfoliated graphene supported on a substrate.[9] Also, graphene nanoelectromechanical devices have great potential for ultrasensitive mass, force and charge sensing.[10,11] Thus motivated, in this Letter, we produce nanomechanical suspended epitaxial graphene (SEG) resonators. Resonance measurements using optical interferometry and nanoindentation using an atomic force microscope (AFM) cantilever are employed to probe the mechanical properties of these doubly clamped structures.

Graphene was grown epitaxially on the silicon face of a chemically mechanically polished 4H-SiC substrate in a sublimation chamber by heating the substrate under a vacuum of $\sim 10^{-5}$ Torr at 1400 °C for 1 h. SiC is chemically a highly resistant material and it is typically patterned using dry etching techniques. However, the plasmas involved in the dry etching process will destroy the graphene and are incapable of undercutting. Hence, a wet etching process was developed to etch the SiC and suspend the graphene.

Doubly clamped structures were defined on graphene using photolithography. A schematic of the fabrication and wet etching process is shown in Figure 1. Fabrication of the devices proceeded by evaporating 100 nm of gold as contact pads, which also served as masks for the wet etch process outlined below. Graphene was then patterned using standard photolithographic techniques and an oxygen plasma etch. The wet etching technique used to etch the SiC followed the photoelectrochemical etching procedure of Kato et al.[12] Aqueous potassium hydroxide (1%) was used as the electrolyte, and the etch was performed at room temperature using a 100 W mercury arc lamp as the source of UV light. The undercut caused by the isotropic etch was sufficient to release the graphene sheets. The current during the etch process was ∼1.2 mA/cm^2 and the etch rate was ∼1 μm/h. The etch was performed for 4 h. The etched area is determined by the spot size of the light source, and the

* Corresponding author, ss626@cornell.edu, 401 Phillips Hall, Cornell University, Ithaca, NY 14853

10.1021/nl900479g CCC: $40.75
Published on Web 08/10/2009

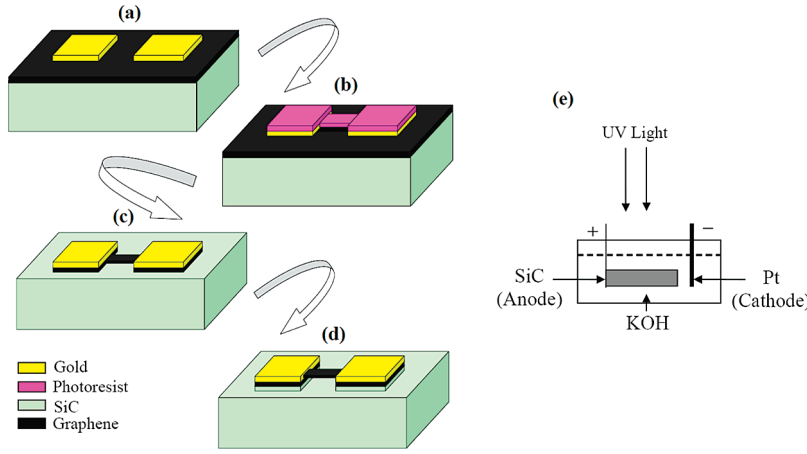

Figure 1. (a−d) Fabrication steps. (a) 100 nm thick gold pads defined photolithographically using lift-off; (b) photoresist patterned over graphene; (c) oxygen plasma etch to define graphene beams and removal of photoresist; (d) photoelectrochemical etching to release the graphene sheets. (e) Schematic of the setup used to perform the SiC etch.

amount of undercut decreases as the light intensity falls off from the center of the focused light spot. Because of the nonuniformity of the light spot, the etch depth over the etched region varies from ∼1 to ∼8 μm, as measured by profilometry. The yield for the devices is 80−90%. To our knowledge, this is the first time a wet etching process has been tried with graphene on SiC. A scanning electron microscope (SEM) image of arrays of doubly clamped SEG devices produced by this technique is shown in Figure 2a. This technique works even for extremely thin (few layer) graphene, as evidenced by the electron transparency of the device shown in Figure 2b. Devices with dimensions ranging from 3 to 20 μm in length and 0.5 to 3.5 μm in width were successfully produced. The thickness of the graphene devices used in this study is estimated to be 1 nm (see Supporting Information). The devices were dried using a critical point drying technique to prevent surface tension-induced breaking.

Raman spectroscopy was performed on the graphene before and after the photoelectrochemical etch process (Figure 2). Raman spectra were collected using a Renishaw InVia micro-Raman system with an excitation wavelength of 488 nm. A blue-shifted G-peak at ∼1587 cm^{-1} and a 2D peak at ∼2719 cm^{-1} are observed for graphene on SiC (after background subtraction). This blue shift has been attributed to compressive strain in the graphene grown on SiC.[13] A disorder-related D peak is barely visible. The Raman spectrum of a SEG device shows the G peak at ∼1580 cm^{-1} and the 2D peak at ∼2707 cm^{-1}. These red-shifts for the suspended graphene are consistent with the hypothesis that registry with the substrate is the cause of the original blue shift. After the etch, a prominent D peak is observed at ∼1354 cm^{-1}. We attribute the D peak to disorder introduced in the graphene either during photolithographic processing or during the etch. However, there is no significant broadening of the G-peak in the suspended devices as has been observed for graphene oxide or functionalized graphene.[14] Thus, we conclude that the chemical structure of the graphene has not been adversely affected by the etching procedure.

AFM images and close-up SEM images of the SEG resonators in Figure 3 show that the resonators are buckled along their lengths. AFM line profiles along the lengths of two of the devices in Figure 3(a)-(b) provide a sample of the different configurations assumed by the buckled beams. The buckled shapes in the figure have been fit using sinusoidal waveforms. Indeed, epitaxial graphene on SiC is under compressive stress, as evidenced from the blue shifts in the Raman spectra.[13] The strain is given by $\varepsilon = (\Delta\omega/\omega)/\gamma$, where $\Delta\omega$ is the change in Raman wavenumber from the unstrained value ω, and γ is the Grüneisen parameter, which is ∼1.8 and ∼2.7 for the G and 2D modes, respectively.[15] The calculated value of the strain for our devices is ∼0.2%. The corresponding compressive stress is orders of magnitude higher than the critical buckling load for the SEG resonators (see Supporting Information). Hence, we expect the graphene beams to be buckled. In addition, Figure 3c shows that the SEG resonators have "side-flanges" and curvature along the width, that make their cross sections look roughly like those of inverted U-channel beams. Also, many devices have local crinkles, as annotated in Figure 3d.

Mechanical resonance measurements were performed at room temperature under vacuum (∼10^{-6} Torr) using an optical actuation and detection technique identical to that described elsewhere.[11,16] In this technique, the intensity of a blue diode laser (405 nm) focused on the device is modulated at a known frequency, leading to periodic thermal expansion and contraction of the graphene layers. This motion of the graphene is detected using reflected light from a red laser (633 nm) coupled to a fast photodiode. The fundamental resonance mode, f_o, for a doubly clamped beam under no tension is given by[17]

$$f_o = A\left[\left(\frac{E}{\rho}\right)\left(\frac{t^2}{L^4}\right)\right]^{1/2} \quad (1)$$

where E is the Young's modulus, ρ is the mass density, t and L are the thickness and length of the beam respectively, and the clamping coefficient, A, is 1.03. For micrometer-sized graphene beams with lengths in the range 3−20 μm and thickness of 1 nm, eq 1 predicts fundamental modes in

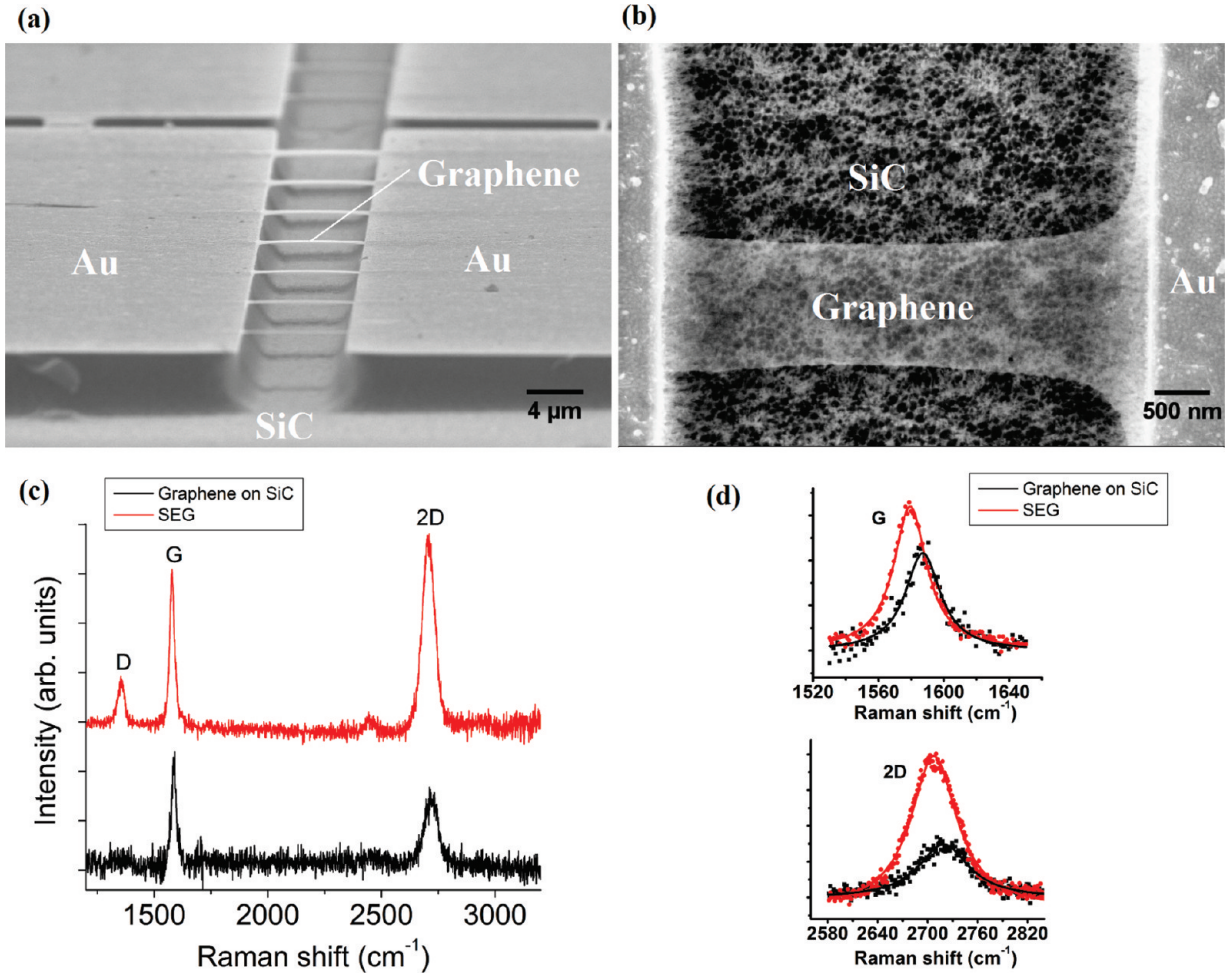

Figure 2. (a, b) Scanning electron microscope images of suspended epitaxial graphene (SEG). (a) An array of doubly clamped nanomechanical graphene beams of length 8 μm and widths ranging from 0.5 to 3.5 μm. The beams are clamped down on both ends by gold pads. (b) Top view of a SEG resonator, showing its electron transparent nature at an electron beam energy of 5 keV. (c, d) Raman spectra of graphene grown on SiC (after background subtraction) and suspended epitaxial graphene (SEG). Data for graphene on SiC are shown in black, and data for SEG are shown in red. G, 2D, and D peaks are seen. The spectrum for the SEG is red-shifted as clearly shown by the zoomed-in spectra in (d). Also, we note that the 2D peak of SEG is fit well by a single Lorentzian.

the range 55 kHz to 2.4 MHz. Figure 4 shows the measured frequencies for SEG devices of different lengths. The inset shows the measured resonance for a sample device. Q factors in the range of 50−400 were observed for most devices. Also plotted in Figure 4 are the resonances expected from eq 1. The measured resonance frequencies are much higher than those predicted by eq 1. Built-in tension is one of the factors responsible for increased frequencies in graphene resonators.[11,18] However, as discussed earlier, the SEG resonators are not under tension and instead are buckled. We hypothesize that their inverted U-shaped cross section contributes to their increased rigidity. A model calculation showing how the U-shaped cross section could explain the increased resonance frequency for a device is included in the Supporting Information. The scatter of the data for the SEG resonators suggests that the resonance frequency of the devices depends strongly upon the local geometry. The variability in the configuration of buckled beams, local crinkling, and the inverted U-shaped cross section do not lend themselves easily to analytical modeling. Accurately predicting the resonant frequencies for the devices would require knowledge of the local geometry from a combination of AFM and SEM images and the residual stress in the devices postbuckling. Then, a finite-element analysis, similar to the one performed by Robinson et al.,[19] would be needed to calculate the vibrational modes of the devices.

In order to remove possible photoresist residues, the suspended devices were then annealed in an Ar/H_2 atmosphere (Ar/H_2 flow rates 400/600 sccm) at 400 °C for 1 h.[20] However, the annealing process destroyed many of the devices. The rupture could have been a result of either the high gas flow rates or thermal mismatch/adhesion issues between the gold contact pads and graphene. The SEG resonators that survived the anneal were again probed using laser interferometry. The frequencies of all SEG resonators went up postanneal (Figure 5a). Also, Q factors close to 10^3 were observed for some devices (Figure 5b). Figure 5c shows SEM images of the same device before and after the annealing process. The reduction in the length of the side-flanges suggests increased tension in the annealed devices. Increased tension and possible residue removal could account for the higher frequencies and Q factors postanneal.

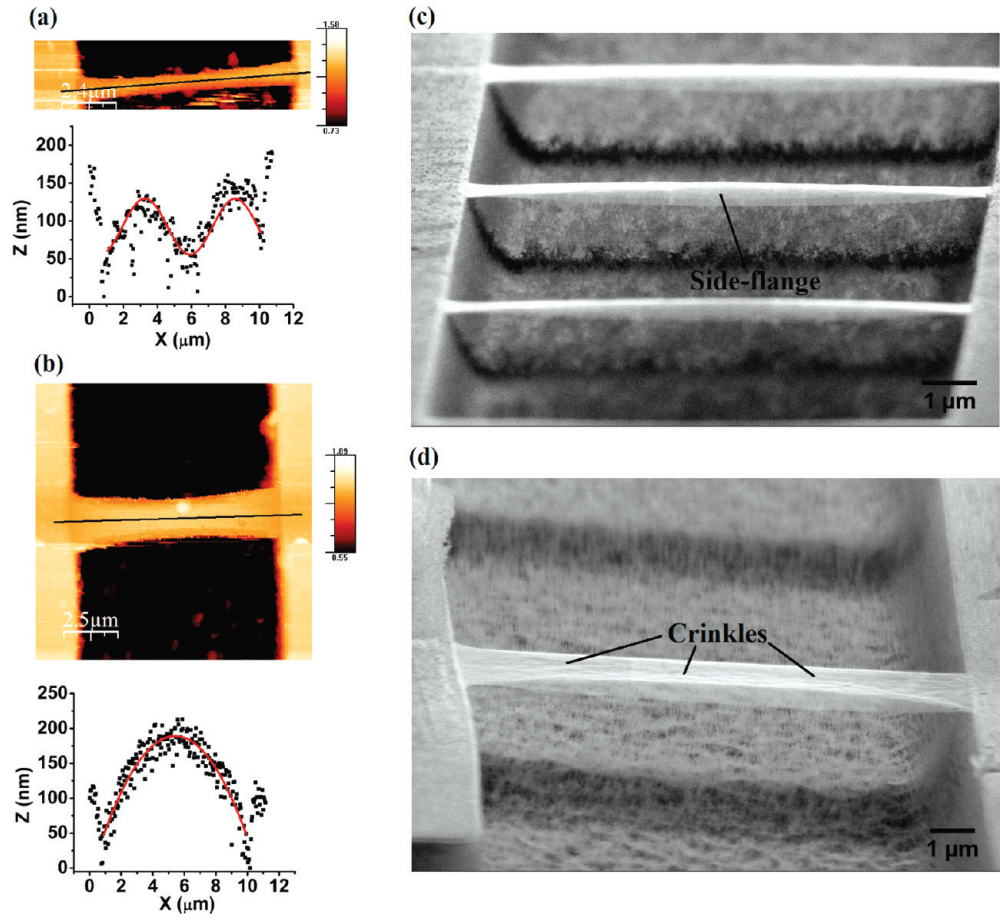

Figure 3. (a, b) AFM images of two SEG devices, showing the variability in configuration of the buckled beams. The shapes of the beams have been fit using sinusoidal waveforms. (c, d) SEM images of SEG devices, showing their buckled nature. The side-flanges and curvature along the width giving rise to a roughly inverted U-shaped cross section and local crinkling are annotated.

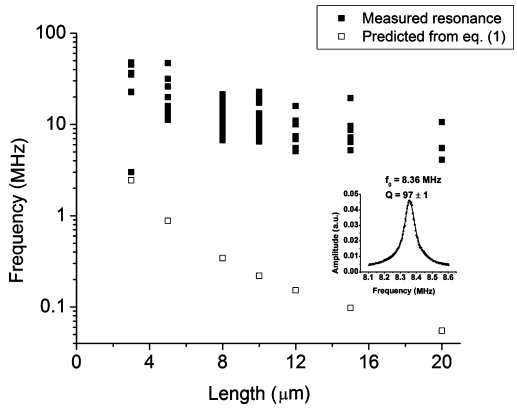

Figure 4. Plot of resonances of devices of various lengths measured using laser interferometry. The measured data are shown using filled squares. The frequencies expected from standard theory for a flat beam with no tension are plotted using hollow squares. Inset shows measured resonance of a sample device with length 8 μm.

Finally, a calibrated AFM cantilever was used to probe the local stiffness of the devices following the anneal. A schematic of the nanoindentation experiment is shown as an inset in Figure 6. In this experiment, the cantilever tip is pushed against the center of the suspended sheet in the tapping mode. As soon as the tip makes contact with the graphene, the free amplitude of vibration of the cantilever goes to zero. The applied force of the cantilever tip against the sheet causes the tip to deflect and also causes the sheet to bend. The tip displacement, the piezo displacement, and the bending of the graphene sheet are related by $z_{piezo} = z_{graphene} + z_{tip}$, where the positive z-axis points downward and all distances are measured along it. Figure 6a presents force−deflection curves for one of the SEG devices that displayed reproducible behavior using multiple cantilevers (see Supporting Information). The low-force portion of the nonlinear force−displacement curves may be fit by a linear spring constant K_1. It is seen that K_1 is much larger than the spring constant expected from standard beam theory for beams under no tension, K_{beam}, given by[21] $K_{beam} = (32Ewt^3/L^3)$ (Figure 6b). We also compare K_1 with the stiffness deduced from laser interferometry experiments postanneal. The spring constant of the mode excited by optical resonance measurements is given by[22] $K_{opt} = m_{eff}\omega_0^2 = (0.735\rho Lwt)(2\pi f_0)^2$. Comparing K_1 and K_{opt} for the resonators, we find that K_{opt} is greater than K_1 by roughly an order of magnitude. This suggests that local rigidity is lower than global stiffness for these devices, which is indicative of local bending and stretching during the nanoindentation experiments.

In conclusion, we report a method for large-scale production of doubly clamped suspended epitaxial graphene resonators from graphene on SiC by a photoelectrochemical wet

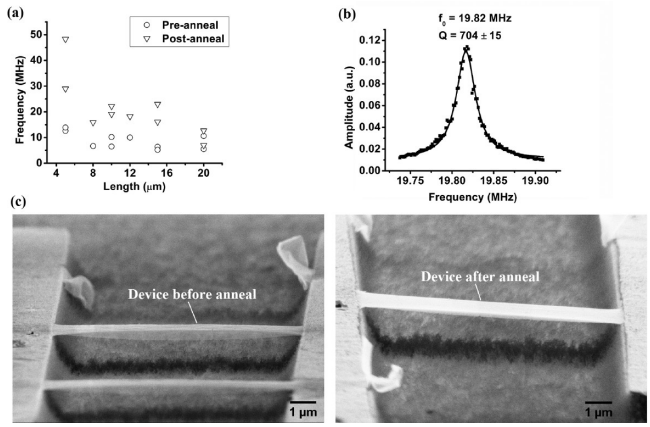

Figure 5. (a) Comparison of resonance frequencies of devices before and after anneal. (b) Measured resonance of a device after anneal. (c) SEM images showing a device before and after anneal.

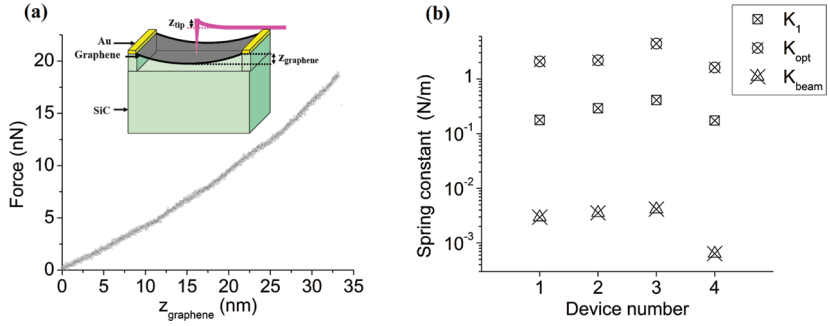

Figure 6. (a) Force-displacement curve for a SEG device. Inset shows schematic of the nanoindentation experiment with an AFM cantilever. z_{tip} and $z_{graphene}$ denote the tip deflection and the displacement of the graphene sheet, respectively. (b) Comparison of low-force nanoindentation spring constant, K_1, with spring constant extracted from the optically actuated resonance mode, K_{opt}, and spring constant expected from standard beam theory for a beam under no tension, K_{beam}.

etch process. The Raman spectrum of the suspended graphene does not suggest extensive chemical modification by the etch. Both optical resonance measurements and nanoindentation experiments show that the nanomechanical SEG resonators are much stiffer than expected on the basis of standard beam theory. This stiffness may be attributed to the buckled and inverted U-shaped cross section of the beams for devices before the Ar/H_2 anneal. Tension may play a role in the increased resonance frequencies of the post-anneal devices. Isolation of epitaxial graphene from the substrate by this technique paves the way for a variety of mechanical, electronic, and optical experiments to probe the true nature of epitaxial graphene without interference of the substrate.

Acknowledgment. We thank A. M. van der Zande for useful technical discussions and C. S. Ruiz-Vargas for the Ar/H_2 anneal. This work is supported by the Cornell Center for Materials Research program of the National Science Foundation (cooperative agreement 0520404) and the Air Force Office of Scientific Research (Contract No. FA9550-07-1-0332, contract monitor Dr. Donald Silversmith).

Supporting Information Available: Details of the thickness of suspended epitaxial graphene (SEG) resonators, critical buckling load for graphene resonators, calculation showing increased resonance frequency of a beam with inverted U-shaped cross section, nanoindentation experiments using AFM cantilever, and figure showing model of a beam with an inverted U-shaped cross section and SEM image of a SEG resonator device. This material is available free of charge via the Internet at http://pubs.acs.org.

References

(1) Novoselov, K. S.; Geim, A. K.; Morozov, S. V.; Jiang, D.; Zhang, Y.; Dubonos, S. V.; Grigorieva, I. V.; Firsov, A. A. *Science* **2004**, *306*, 666.
(2) Novoselov, K. S.; Jiang, Z.; Zhang, Y.; Morozov, S. V.; Stormer, H. L.; Zeitler, U.; Maan, J. C.; Boebinger, G. S.; Kim, P.; Geim, A. K. *Science* **2007**, *315*, 1379.
(3) Rana, F. *IEEE Trans. Nanotechnol.* **2008**, *7*, 91.
(4) Liang, G.; Neophytou, N.; Nikonov, D. E.; Lundstrom, M. S. *IEEE Trans. Electron Devices* **2007**, *54*, 657.
(5) Williams, J. R.; DiCarlo, L.; Marcus, C. M. *Science* **2007**, *317*, 638.
(6) Lemme, M. C.; Echtermeyer, T. J.; Baus, M. Kurz, H. *IEEE Electron Device Lett.* **2007**, *28*, 282.
(7) Schedin, F.; Geim, A. K.; Morozov, S. V.; Hill, E. W.; Blake, P.; Katsnelson, M. I.; Novoselov, K. S. *Nat. Mater.* **2007**, *6*, 652.
(8) Bunch, J. S.; Verbridge, S. S.; Alden, J. S.; van der Zande, A. M.; Parpia, J. M.; Craighead, H. G.; McEuen, P. L. *Nano Lett.* **2008**, *8*, 2458.
(9) Bolotin, K. I.; Sikes, K. J.; Jiang, Z.; Klima, M.; Fudenberg, G.; Hone, J.; Kim, P.; Stormer, H. L. *Solid State Commun.* **2008**, *146*, 351.
(10) Sakhaee-Pour, A.; Ahmadian, M. T.; Vafai, A. *Solid State Commun.* **2008**, *145*, 168.
(11) Bunch, J. S.; van der Zande, A. M.; Verbridge, S. S.; Frank, I. W.; Tanenbaum, D. M.; Parpia, J. M.; Craighead, H. G.; McEuen, P. L. *Science* **2007**, *315*, 490.
(12) Kato, M.; Ichimura, M.; Arai, E.; Ramasamy, P. *Jpn. J. Appl. Phys.* **2003**, *42*, 4233.

(13) Ferralis, N.; Maboudian, R.; Carrazo, C. *Phys. Rev. Lett.* **2008**, *101*, 156801.
(14) Kudin, K. N.; Ozbas, B.; Schniepp, H. C.; Prud'homme, R. K.; Aksay, I. A.; Car, R. *Nano Lett.* **2008**, *8*, 36.
(15) Mounet, N.; Marzari, N. *Phys. Rev. B* **2005**, *71*, 205214.
(16) Ilic, B.; Krylov, S.; Aubin, K.; Reichenbach, R.; Craighead, H. G. *Appl. Phys. Lett.* **2005**, *86*, 193114.
(17) Weaver, W.; Timoshenko, S. P.; Young, D. H., *Vibrations Problems in Engineering*; Wiley: New York, 1990.
(18) Frank, I. W.; Tanenbaum, D. M.; van der Zande, A. M.; McEuen, P. L. *J. Vacuum Sci. Technol., B* **2007**, *25*, 2558.
(19) Robinson, J. T.; Zalalutdinov, M.; Baldwin, J. W.; Snow, E. S.; Wei, Z.; Sheehan, P.; Houston, B. H. *Nano Lett.* **2008**, *8*, 3441.
(20) Ishigami, M.; Chen, J. H.; Cullen, W. G.; Fuhrer, M. S.; Williams, E. D. *Nano Lett.* **2007**, *7*, 1643.
(21) Senturia, S. D., *Microsystem Design*; Kluwer Academic Publishers: Norwell, MA, 2001.
(22) Ekinci, K. L.; Roukes, M. L. *Rev. Sci. Instrum.* **2005**, *76*, 061101.

NL900479G